Review

Research Progress on the Sintering Techniques of Zirconia in Prosthetic Dentistry

Chuyue Yang and Xiaoqiang Liu *

Department of Prosthodontics, Peking University School and Hospital of Stomatology & National Center for Stomatology & National Clinical Research Center for Oral Diseases & National Engineering Research Center of Oral Biomaterials and Digital Medical Devices, Beijing 100081, China; yangchuyue@stu.pku.edu.cn
***** Correspondence: liuxiaoqiang@bjmu.edu.cn

Abstract

Zirconia is widely used in prosthodontics due to its excellent biocompatibility, mechanical properties, and esthetic characteristics. This article reviews the fundamentals of sintering zirconia for prosthodontic applications. Various sintering techniques, including conventional, spark plasma, high-speed, and microwave sintering, are discussed regarding their influence on translucency, strength, and microstructure. This review aims to provide a comprehensive reference for the sintering methods of zirconia currently used or may be used for dental prosthodontics.

Keywords: zirconia; sintering; crystalline; optical properties; mechanical properties

1. Introduction

Zirconia has become the cornerstone restorative material of contemporary dentistry [1]. Fabrication of zirconia prostheses involves subtractive or additive manufacturing of oversized green bodies in dental laboratories. This is followed by a precisely calibrated sintering protocol that induces controlled volumetric shrinkage, achieving accurate adaptation to tooth preparations [2].

Pure zirconia, with a melting point of approximately 2700 °C [2], exhibits three crystal phases (Figure 1), of which the monoclinic (M) phase is stable below 1170 °C; the tetragonal (T) phase stable from 1170 °C to 2370 °C; and the cubic (C) phase stable from 2370 °C to the melting point [3–5]. The phase transitions from tetragonal or cubic to monoclinic polymorphs are accompanied by a significant volume expansion (3–5%) that induce catastrophic failure of pure zirconia. To mitigate this, stabilizing oxides such as MgO, CaO, Y_2O_3, Al_2O_3, or CeO_2 are added in solid solution to reduce the martensitic transformation temperature below the ambient [6,7]. This enables retention of the metastable tetragonal and cubic phases after sintering [3].

The zirconia microstructure (grain size, density, and uniformity) is controlled by the composition and sintering parameters. Such structural characteristics govern the optical and mechanical properties [8,9]. This review examined conventional, spark plasma, high-speed, and microwave sintering techniques. Achieving high strength and toughness remains critical for dental prostheses, requiring optimized sintering methods.

room temperature to 1170°C   *1170°C to 2370°C*   *2370°C to melting point*

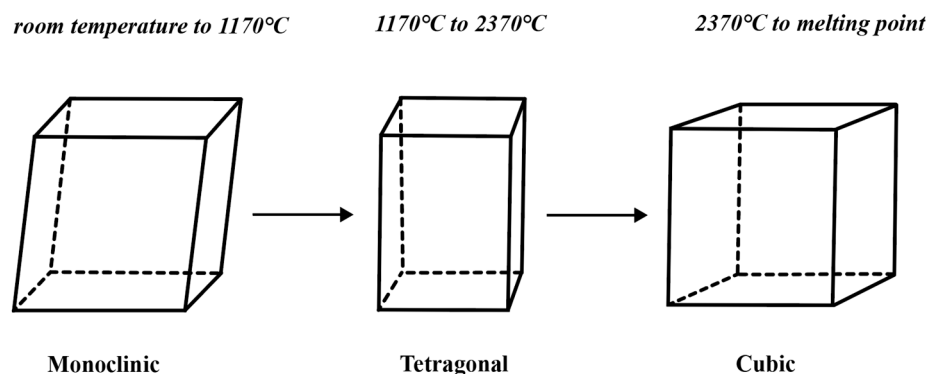**Monoclinic**   **Tetragonal**   **Cubic**

Figure 1. Crystal forms of pure zirconia with the transformation temperatures.

2. Fundamentals of Sintering

Sintering consolidates powders into dense solids [10]. The key parameters governing sinterability and microstructure are the material properties (particle size and composition) and the process variables (the heating method, temperature, time, pressure, atmosphere, and the heating/cooling rates) [10]. The final properties are primarily dictated by the thermodynamic principles [11–13] that govern densification and grain size coarsening [10].

Classical sintering theory models molecular diffusion in compact powders using spherical particles [14]. Five atomic transport mechanisms are in operation: evaporation and solidification, surface diffusion, grain boundary diffusion, volume diffusion, and plastic deformation [15]. Crucially, grain boundary diffusion, volume diffusion, and plastic deformation induce densification [16]; the other mechanisms only reduce the surface area.

Surface energy minimization is the primary force that drives sintering [10]. Densification is usually accompanied by grain growth. Intracrystalline domains coarsen, further lowering the surface energy (Figure 2). Sintering occurs at temperatures exceeding 50% of the absolute melting point, characterized by interparticle neck formation [17,18] (Figure 3a). Densification progresses through three stages—initial, intermediate, and final—defined by the neck-to-particle diameter ratio (X/D) [16].
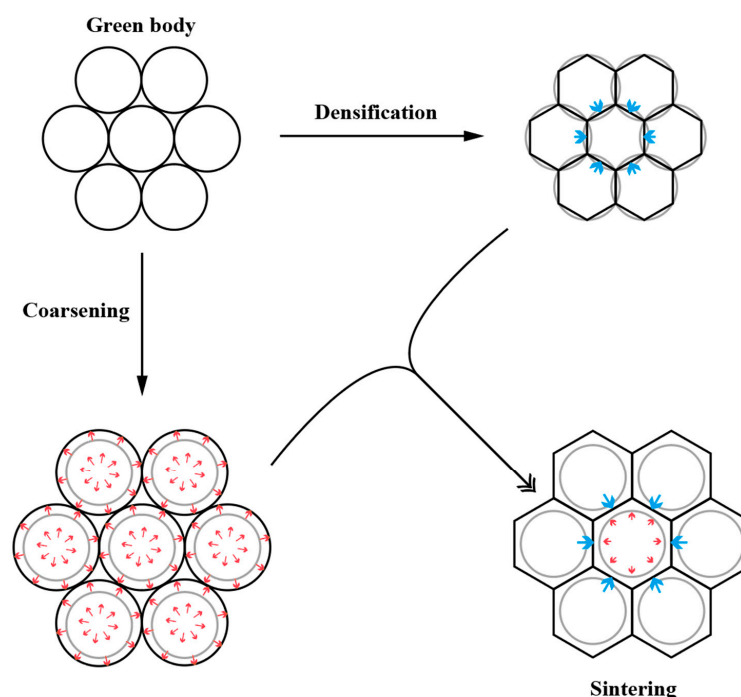
Figure 2. Fundamental phenomena occur during sintering (red arrows: crystal growth; blue arrows: densification) [10].
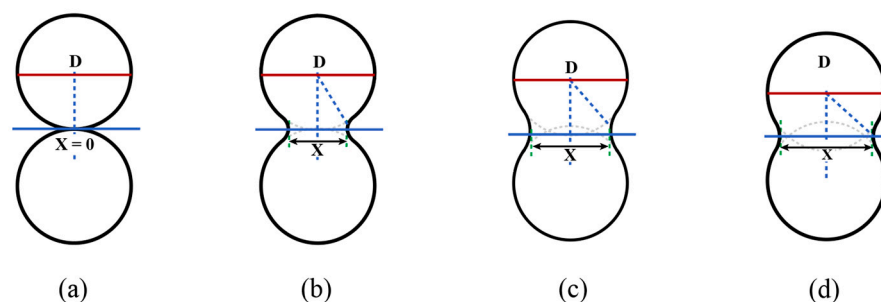
Figure 3. The two-particle model for the initial stage of sintering. (**a**) Point-to-point contact. (**b**) The initial stage, X/D < 0.3. (**c**) The intermediate stage, 0.3 ≤ X/D ≤ 0.7. (**d**) The final stage, X/D > 0.7.

Initially, X/D < 0.3 interconnected pore networks enable active densification [19] (Figure 3b). The intermediate stage (0.3 ≤ X/D ≤ 0.7) [18] features a transition to isolated closed porosity [19] (Figure 3c). In the final stage (Figure 3d), activation at X/D > 0.7 induces grain boundary curvature-driven pore encapsulation. Curved boundaries expand the interfacial area to entrap residual pores [19,20]. Densification slows, and the sintering dynamics shift toward diffusion-limited grain coarsening [10]. Ostwald ripening preferentially dissolves smaller grains that are then re-deposited on larger grains [21,22].

3. Sintering Techniques

Many sintering methods have been used to densify zirconia, ranging from conventional radiant heating to field-assisted sintering that exploits the Joule heating principles [21–23]. Rapid sintering enhances production efficiency in dental laboratories that must meet tight clinical turnaround requirements. Microwave sintering [24–26] and spark plasma sintering [27–29] optimally fabricate dental zirconia prostheses. This section elaborates on variants of these processes (Figure 4). Novel techniques reduce the processing time with retention of high zirconia flexural strength [30,31]. Advanced sintering technologies enable the fabrication of restorations exhibiting excellent biomechanical performance and natural esthetic gradation.
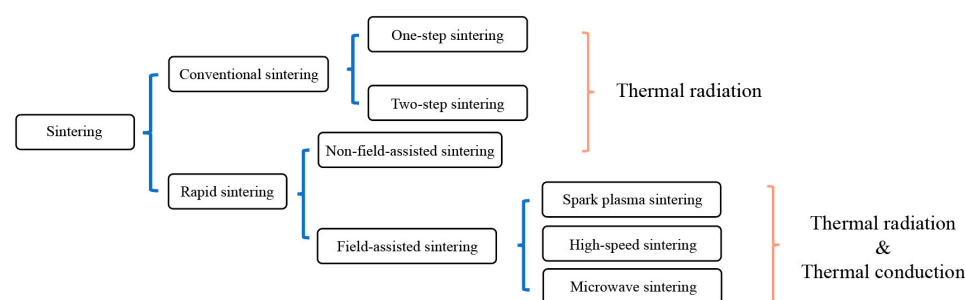

Figure 4. Sintering methods of zirconia.

3.1. Conventional Sintering

Conventional sintering of zirconia uses radiant heating in resistance ovens/furnaces with gradual ramp rates up to 1450 °C to 1500 °C [32,33]. The material is isothermally held at the top temperature for 2 to 4 h, followed by furnace cooling [33]. However, prolonged exposure at 1150 °C induces abnormal grain growth, degrading the flexural strength and fracture toughness of a 3 mol% yttria-stabilized tetragonal zirconia polycrystal (3Y-TZP) [34,35].

In 2000, Chen et al. proposed a two-step sintering process for nanocrystalline ceramics, which was later used to prepare Y-TZP and was optimized by Grech et al. [36]. A short dwell (about 1 min) at the peak temperature (T_1) was followed by rapid reduction to a lower temperature (T_2) at which an extended (from 5 to 20 h) isothermal hold was performed

before further cooling [37–39]. The selection of two holding temperatures minimized nano-sized grain growth and enhanced densification. At T_1, the thermodynamic driving force allowed grain boundary diffusion and densification. The lower T_2 restricted grain growth, but permitted further densification [33,37,40]. The relationship between the reaction rate constant (k), activation energy (E_a), and temperature (T) can be expressed by an Arrhenius equation with the constant R:

$$k = A \cdot e^{-\frac{Ea}{RT}},\qquad(1)$$

$$lnk = -\frac{Ea}{R} \cdot \frac{1}{T} + lnA,\qquad(2)$$

Figure 5 shows the linear relationship, the logarithm of the reaction rate constant (k), and the activation energies for densification (E_d) and grain growth (E_g). In a system wherein the activation energy for densification exceeds that for grain growth [41], T_1 and T_2 values that inhibit grain growth can always be chosen.
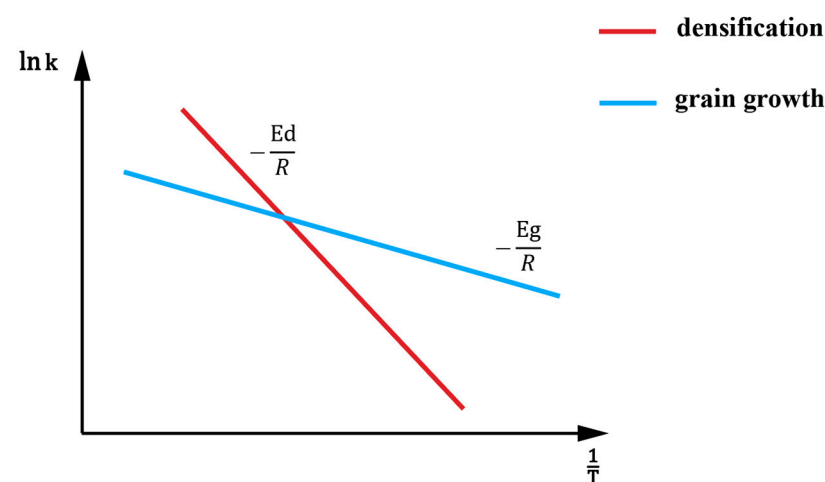

Figure 5. The temperature dependencies of material densification and grain growth rates when the activation energy for densification (E_d) exceeds that for grain growth (E_g) [42,43].

Other studies used two-step sintering of zirconia dental prosthetics; the approximate temperature ranges for T_1 and T_2 were 1450 to 1550 °C and 1250 to 1350 °C [33]. Two-step sintering is associated with a higher density and a finer grain size than one-step sintering, yielding a more uniform microstructure. T_1 primarily affects grain size; the impact on density is minimal. T_2 primarily influences density, with little effect on grain size [33].

3.2. Rapid Sintering

3.2.1. Non-Field-Assisted Sintering

Speed sintering (SS) requires 30 to 120 min and can proceed chairside in a single visit. SS utilizes a conventional furnace. Such a furnace generates heat at a faster rate (~40 to 70 °C/min) by featuring a smaller heating chamber [44]. Julia et al. [45] developed a generalized speed-sintering program for typical sintering furnaces with electrically resistive heating elements. Ramp heating at 17 °C/min was followed by holding for 35 min at 1540 °C, cooling at 18 °C/min to 1200 °C, and at 35 °C/min thereafter. However, optimal rapid sintering of existing zirconia materials has not been well studied. More data is required.

3.2.2. Field-Assisted Sintering

Field-assisted sintering drives material transport by coupling external pressure and field to reduce the activation energy required for diffusion [41,46]. This reduces the sintering time and temperature, and accelerates densification [41,46].

Spark Plasma Sintering

Spark plasma sintering, also termed pulsed current sintering [41], uses pulsed direct current (DC) and uniaxial pressure [47,48]. Pulse discharge is combined with rapid thermal, electrical, and mechanical heating [46,49]. The equipment (Figure 6) features electrodes that deliver stable pulsed currents and an external mold with bilateral punches. Typically, graphite is employed to maintain the pressure at less than 100 MPa within a reducing or inert gas atmosphere [27,28]. Conductive powders are activated by a pulsed voltage, followed by DC that induces densification via Joule heating [46].
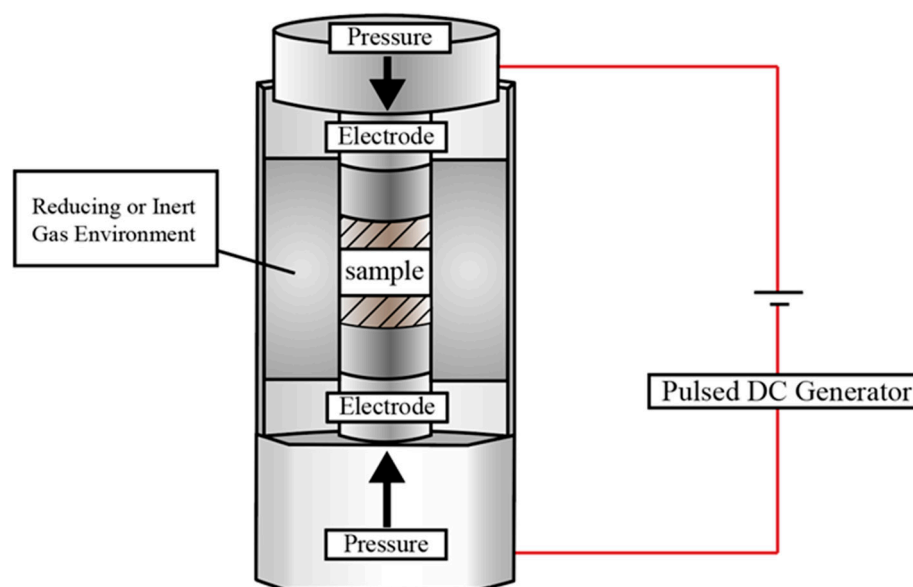

Figure 6. Schematic of a spark plasma sintering apparatus [49].

Yang et al. [50] studied spark plasma sintering of zirconia ceramics. This produced uniform grains and maintained the tetragonal phase, as do conventional sintering methods. The mechanical and optical properties of the final products did not differ significantly from those of conventional materials. The sintering time fell from 8 h of the conventional process to 2 h, and energy consumption was reduced, productivity enhanced. [50]. However, current spark plasma sintering techniques cannot be used to prepare fixed prosthodontics fabricated from dental zirconia. These require customized dies that shape the crowns. The dies introduce thermal gradients that may trigger thermal shock in the sintered body [51]. The effects of spark plasma sintering on crown production and properties have not been studied.

Induction Sintering

Induction heating has been used to sinter some forms of zirconia [32]. An alternating electromagnetic field generates a current that volumetrically heats a material (Figure 7). During initial sintering, the zirconia specimen is placed in the center of the device [52]. After the initial heating, the electrical conductivity of zirconia increases. Then, the alternating magnetic field induces an electromagnetic current, allowing faster heating [52]. The induction furnace can sinter a zirconia crown in 18 to 30 min [53]. Most commercial dental zirconia products exhibit higher flexural strength when induction-heated for 10 min at 1580 °C than do conventionally sintered materials [22,53–55]. Lee et al. [56] investigated the effects of induction sintering on the marginal and internal fits of monolithic zirconia crowns from a macroscopic viewpoint. Compared with conventional sintering, the marginal discrepancy diminished during induction sintering of zirconia crowns, and the internal fit remained satisfactory [56].
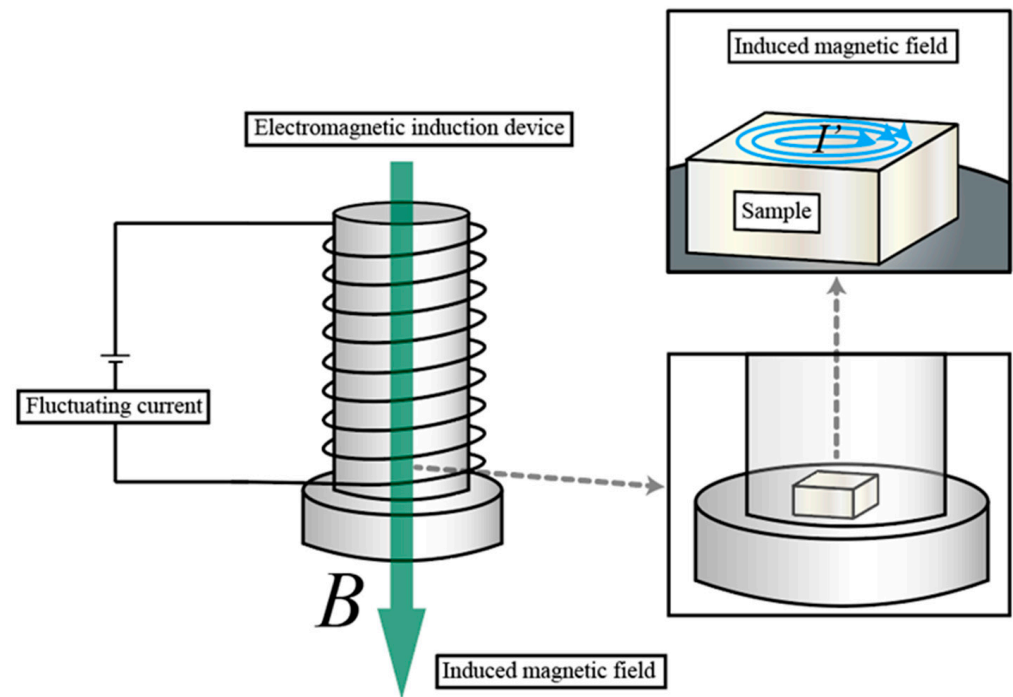
Figure 7. Schematic of the structure and principle of high-speed furnace sintering [31].

Microwave Sintering

Microwave sintering uses volumetric microwave absorption, not radiant surface-limited heat transfer [57]. This bypasses the thermal conductivity constraints via dielectric coupling with electromagnetic fields [57]. Since the 1980s, microwave processing has been used to densify oxide ceramics [58,59].

Binner et al. [60] developed a hybrid microwave/conventional furnace operating in either a single mode (pure microwave) or a dual mode (microwave and radiation). Microwave power was applied at 600 W for rapid heating to T_1 (Figure 8), and the radiant power was varied when creating the T_2 cooling profile of two-step sintering [60].
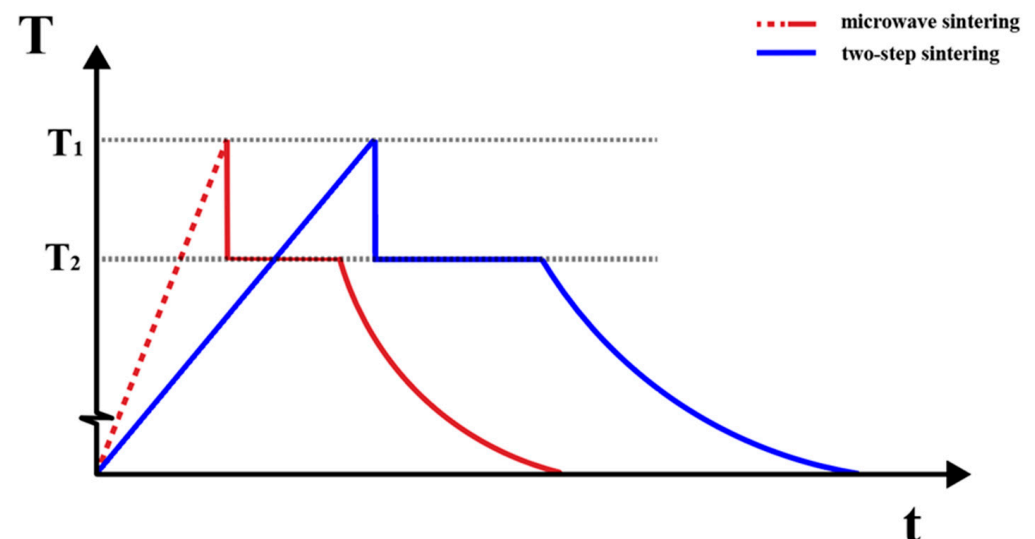

Figure 8. The temperature-time curve of conventional two-step sintering is similar to that of multimode microwave sintering, but the time to temperature is much shorter. (T: heating temperature; t: heating time) [60].

Compared to conventional sintering, microwave sintering enables rapid densification by accelerating the kinetics of many processes in ceramic, polymeric, and organic systems, overcoming impediments to grain growth via dipole polarization and interfacial friction heating [61,62]. The dielectric heterogeneity of polydisperse grains and impurities induces nonlinear polarization and local variations in the loss tangent, triggering thermal runaway wherein absorption outpaces dissipation. Differential thermal expansion of multicomponent systems further amplifies microstructural defects, ultimately degrading the flexural strength and fatigue resistance of dental zirconia prostheses. Microwave sintering remains under exploration [61,62].

4. Effects of Sintering Methods on Properties

Sintering is accelerated when various field energies increase the heating rate and minimize the holding time [10,46]. The sintering parameters affect the properties of zirconia ceramics, including grain size, the phase transitions, mechanical strength, and the optical characteristics [54,63]. The impacts of different conditions on the mechanical and esthetic properties vary [52,64]. This section summarizes the effects of sintering conditions on zirconia ceramics.

4.1. Optical Performance

The esthetic quality of zirconia restorations depends on the optical properties, including translucency, the contrast ratio, color, and opalescence [65,66]. The light transmittance of a 3Y-TZP is reduced by scattering at the grain boundaries, pores, and secondary phases [22,67]. Higher sintering temperatures reduce porosity and enhance density, minimizing light scattering and improving translucency [44,68]. Kamal et al. [68], Jiang et al. [69], and Stawarczyk et al. [55] found that translucency increased at higher sintering temperatures (1300 to 1700 °C). Fast-sintered zirconia shows slightly superior optical properties compared to conventionally sintered materials, and two-step sintering is better than single-step procedures [55,68,69].

Marina et al. [44] compared conventional sintering (1510 °C with a hold for 4 h), spark plasma sintering (1510 °C with a hold for 60 min), and fast sintering (1580 °C with a hold for 10 min). The latter procedure exhibited the highest translucency and the smallest grain size [22,44,54].

Microwave sintering in a high-temperature furnace (Sintramat; Ivoclar Vivadent, Buffalo, NY, USA) produces zirconia of lower porosity and more uniform grain size than conventional methods, improving light reflection and hue [22,70]. Transparency can be enhanced by adding various metal oxides that change the phase transition temperature range of zirconium dioxide and modify the grain boundary chemistry to reduce secondary phases and porosity [44,67]. The meta-analysis of Liu et al. [66] revealed negligible differences in the CIEDE2000 transparency and contrast ratio between fast/conventional sintering, and a higher CIE L*a*b* transparency of conventionally sintered Y-TZP than other materials.

4.2. Crystal Stability

Zirconia can be divided into partially stabilized zirconia (PSZ), tetragonal zirconia polycrystalline (TZP), and fully stabilized zirconia (FSZ) [71]. A higher cubic phase content enhances translucency but reduces flexural strength and fracture toughness [72,73]. The phase composition is critical in terms of the mechanical properties.

Mahinour et al. [30] reported that high-speed sintering reduced the tetragonal phase and increased the monoclinic phase. The sintering method, particularly field-assisted sintering, significantly influenced the phase transformation kinetics by lowering the sintering temperature threshold. Huang et al. [71] studied Al_2O_3-doped zirconia that was microwave

sintered. The initial 4 mol% Al_2O_3-ZrO_2 powder contained monoclinic and tetragonal phases [71]. After sintering, diffraction peaks of α-Al_2O_3 and c-ZrO_2 were apparent, indicating enhanced phase stability of these specific compositions [71]. This illustrates how both dopants and the sintering method synergistically influence the phase evolution of even non-dental systems. This implies that zirconia stabilized by various metal oxides may exhibit distinct phase behaviors and material properties, encouraging future research on zirconia optimization for dental and other biomedical applications.

4.3. Microstructure

Ji et al. [74] studied 3Y-TZP ceramics sintered at 5 °C/min. At 1000 °C, the grain size matched the dimensions of the initial powder particles despite rearrangement of the particle clusters. At 1200 °C, grain growth and neck formation created continuous pore networks as rearrangement progressed [74]. Above that temperature. neighboring grains coalesced, forming a distinctive connected porosity [17,74]. Specimens sintered at 1300 °C exhibited abnormal grain growth with localized oversized grains [74]. Further heating to 1500 °C eliminated residual pores, increased the average grain size to 522.65 nm, and achieved full densification [17,74]. Mahinour et al. [30] observed that the tetragonal phase proportions in fast-sintered (heating and cooling at higher than 50 °C/min) zirconia were consistent across various brands. The existing experimental data do not reveal the phase transformation patterns of the various sintering methods.

4.4. Mechanical Properties

4.4.1. Flexural Strength

Figure 9 illustrates grain size evolution (Figure 9a) and densification (Figure 9b) of 3Y-TZP ceramics sintered at 800 to 1500 °C [74]. Initially, flexural strength increases with temperature. However, the densification rate declines as grain coarsening progresses. Ostwald ripening of internal voids exacerbates the microstructural homogeneity [75], in turn reducing the mechanical strength. Commercial dental zirconias come with manufacturer-recommended sintering protocols that optimize density and strength [55,68,69].
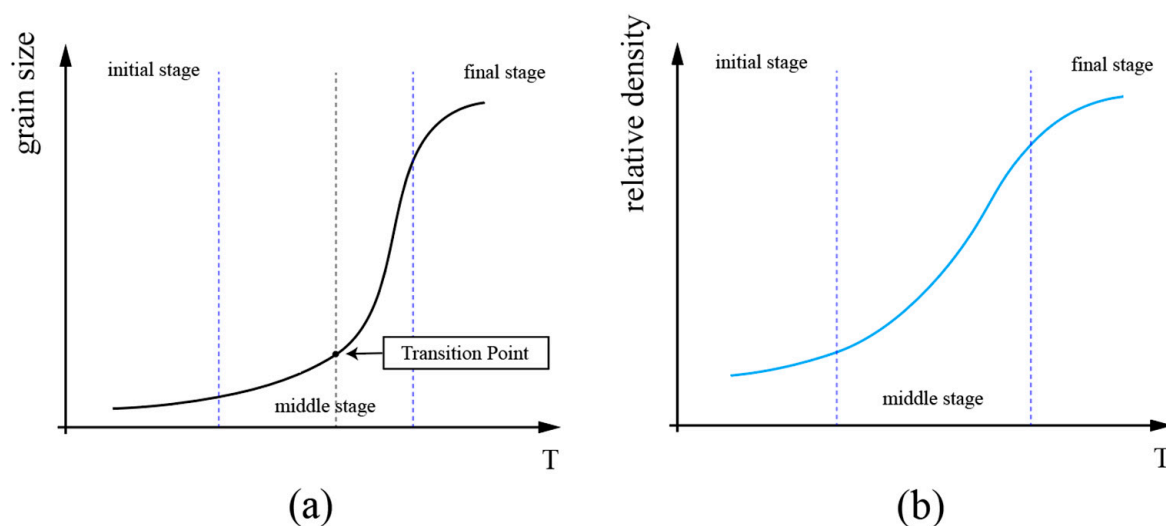

Figure 9. The average grain size (**a**) and relative density (**b**) of 3Y-TZP ceramics during the sintering process (T: Sintering temperature) [74].

Ersoy et al. [63] compared conventional sintering at a fixed rate (to 1510 °C with a hold for 120 min) to two-step sintering (to 1540 °C with a hold for 25 min followed by a rise to 1580 °C with a hold for 10 min). Two-step sintering afforded a marginally higher strength than conventional sintering. The meta-analysis of Liu et al. [65] revealed no

statistically significant differences in translucency, the contrast ratio, flexural strength, or fracture toughness among the sintering methods.

4.4.2. Fracture Toughness

Mustafa et al. [76] divided samples into two groups using the sintering procedures recommended by the manufacturer: a standard group and an accelerated group. Biaxial fracture stress (BFS) testing was performed, and the chemical content, grain size, and phase composition were derived [76]. The two groups exhibited similar crystal structures but slightly different chemical compositions. However, the BFS values differed significantly [76], revealing the impacts of different sintering methods on fracture toughness [77]. The average fracture strength of the standard-sintered group was 1597.93 ± 90.44 MPa, and that of the accelerated-sintered group was 1336.54 ± 114.96 MPa. However, the fracture strength of all samples exceeded the values recommended by the ISO 6872 standard [76].

The 2023 meta-analysis of Liu et al. [65] showed that rapid sintering (compared to conventional sintering) had no significant effect on the three-point bending or biaxial bending strength, or fracture toughness, of YSZ.

4.4.3. Microhardness

Microhardness is a measure of a material's capacity to resist localized plastic deformation associated with the large total grain boundary areas of fine-grained materials. Grain boundaries serve as barriers to dislocation, hindering plastic deformation and increasing resistance to indentation [78]. A finer grain structure increases hardness by more effectively hindering dislocation.

Huang et al. [79] compared ultra-rapid high-temperature sintering (UHS) using an electric field, conventional sintering, and microwave sintering, in terms of microstructure and mechanical properties. Of the three methods, the microwave sample exhibited the highest Vickers hardness (12.16 ± 0.08 GPa) and the UHS sample the lowest (11.05 ± 0.04 GPa) [79]. However, Cokic et al. [80] studied the compositions and physical and mechanical properties (including hardness) of 5Y-PSZ and 3Y-TZP zirconias and found no difference between conventional and fast sintering protocols. Thus, effects do not seem to be systematic or stabilizer-dependent, being rather material-dependent [45]. Literature comparisons of fast sintering methods are not always straightforward because the protocols and materials are study-specific [45].

4.4.4. Low Temperature Degradation

At moderately low temperatures, including those near body temperature (37 °C), and under humid conditions, metastable tetragonal zirconia ceramics are susceptible to a gradual deterioration, a phenomenon known as low-temperature degradation (LTD) [81–84]. LTD represents a critical challenge for stabilized zirconia ceramics in dental applications, as highlighted by Chevalier et al. [82]. Kohal et al. [85] documented a substantial t-m transformation of YSZ implants that had been in the mouth for 3 years up to 15 years, and demonstrated under moist conditions, LTD induces a transformation from the tetragonal to monoclinic phase [86], resulting in microcracking [84], brittle fractures [87], loss of osseointegration, and implant failure [85], with serious health implications. The stability of the tetragonal phase is essential for LTD resistance [88], and it is well established that sintering conditions profoundly influence this stability by modulating microstructural features such as grain size and uniformity [89–91], although the actual role of the pores in triggering low-temperature degradation has not been fully addressed.

Refined microstructures achieved through optimized sintering protocols have been demonstrated to enhance hydrothermal stability by suppressing abnormal grain growth, as evidenced by Sutharsini et al. [92]. Matsui et al. [7] emphasized the critical role of

sintering optimization in mitigating LTD. The work achieved nearly complete suppression of LTD through advanced sintering strategies, including co-doping with Al^{3+} and Ge^{4+} ions, which facilitates precise control of grain boundary nanostructure and improves densification kinetics [7]. Furthermore, in subsequent LTD testing, the 3Y-AG material remained free of LTD after being exposed to hot water at 140 °C for over four years [7]. This approach not only enhances sinterability but also imparts exceptional resistance to LTD [7], highlighting the pivotal function of sintering aids and microstructural engineering in preventing phase transformation and mechanical degradation [92]. These findings affirm that tailored sintering technologies—incorporating stabilizers and optimized processing parameters—are indispensable for improving the durability and reliability of zirconia-based dental prosthetics [91–94].

5. Conclusions

This review analyzed dental zirconia sintering, contrasting conventional and emerging techniques. Although clinical implementations remain few in number, modern radiant heating methods are under active investigation. Field-assisted sintering may increase processing speed and efficiency, preserve translucency, and not compromise crystalline integrity. Fast sintering protocols enable rapid, chairside prosthetic fabrication.

References

1. Grech, J.; Antunes, E. Zirconia in dental prosthetics: A literature review. *J. Mater. Res. Technol.* **2019**, *8*, 4956–4964. [CrossRef]
2. Fedorov, P.P.; Yarotskaya, E.G. Zirconium dioxide. Review. *Kcmf* **2021**, *23*, 169–187. [CrossRef]
3. de Araújo-Júnior, E.N.S.; Bergamo, E.T.P.; Bastos, T.M.C.; Jalkh, E.B.B.; Lopes, A.C.; Monteiro, K.N.; Cesar, P.F.; Tognolo, F.C.; Migliati, R.; Tanaka, R.; et al. Ultra-translucent zirconia processing and aging effect on microstructural, optical, and mechanical properties. *Dent. Mater.* **2022**, *38*, 587–600. [CrossRef]
4. Manicone, P.F.; Rossi Iommetti, P.; Raffaelli, L. An overview of zirconia ceramics: Basic properties and clinical applications. *J. Dent.* **2007**, *35*, 819–826. [CrossRef] [PubMed]
5. Hajhamid, B.; Bozec, L.; Tenenbaum, H.; De Souza, G.; Somogyi-Ganss, E. Effect of artificial aging on optical properties and crystalline structure of high-translucency zirconia. *J. Prosthodont.* **2024**, *33*, 61–69. [CrossRef] [PubMed]
6. Piconi, C.; Maccauro, G. *Zirconia as a Ceramic Biomaterial*; Elsevier Ltd.: Oxford, UK, 1999; Volume 20, pp. 1–25.
7. Matsui, K.; Yoshida, H.; Ikuhara, Y. Nanocrystalline, ultra-degradation-resistant zirconia: Its grain boundary nanostructure and nanochemistry. *Sci. Rep.* **2014**, *4*, 4758. [CrossRef] [PubMed]
8. Borrell, A.; Salvador, M.D.; Rayón, E.; Penaranda-Foix, F.L. Improvement of microstructural properties of 3y-TZP materials by conventional and non-conventional sintering techniques. *Ceram. Int.* **2012**, *38*, 39–43. [CrossRef]
9. Faeghinia, A.; Ebadzadeh, T. Effect of microwave conditions on sintering of hydroxyapatite ceramics. *Sci. Sinter.* **2020**, *52*, 469–479. [CrossRef]
10. Kang, S.L. *Sintering: Densification, Grain Growth and Microstructure*; Elsevier Butterworth-Heinemann: Oxford, UK, 2005.
11. Juntavee, N.; Attashu, S. Effect of different sintering process on flexural strength of translucency monolithic zirconia. *J. Clin. Exp. Dent.* **2018**, *10*, e821–e830. [CrossRef] [PubMed]
12. Khaledi, A.A.R.; Vojdani, M.; Farzin, M.; Pirouzi, S. The effect of sintering program on the compressive strength of zirconia copings. *J. Dent.* **2018**, *19*, 206–211.

13. Ahmed, W.M. Evaluation of Distortion of Monolithic Zirconia Crowns Under the Influence of Different Preparation Designs and Sintering Techniques. Ph.D. Thesis, The University of British Columbia, Vancouver, BC, Canada, 2019.

14. Olevsky, E.A. Theory of sintering: From discrete to continuum. *Mater. Sci. Eng. R Rep. Rev. J.* **1998**, *23*, 41–100. [CrossRef]

15. Lu, K. *Nanoparticulate Materials: Synthesis, Characterization, and Processing*; John Wiley & Sons, Inc.: Hoboken, NJ, USA, 2013.

16. Lu, K. Sintering of nanoceramics. *Int. Mater. Rev.* **2008**, *1*, 21–38. [CrossRef]

17. Yin, Y.; Xu, J.; Ji, M.; Li, L.; Chen, M. A critical review on sintering and mechanical processing of 3y-TZP ceramics. *Ceram. Int.* **2023**, *49*, 1549–1571. [CrossRef]

18. Mazlan, M.R.; Jamadon, N.H.; Rajabi, A.; Sulong, A.B.; Mohamed, I.F.; Yusof, F.; Jamal, N.A. Necking mechanism under various sintering process parameters—A review. *J. Mater. Res. Technol.* **2023**, *23*, 2189–2201. [CrossRef]

19. Ferrage, L.; Bertrand, G.; Lenormand, P. Dense yttria-stabilized zirconia obtained by direct selective laser sintering. *Addit. Manuf.* **2018**, *21*, 472–478. [CrossRef]

20. Balod, A.O.; Al Sarraf, Z.; Mattie, A.A. Determination of the neck size between powders during sintering process using finite element methods. *JoCEF* **2020**, *1*, 29–36. [CrossRef]

21. Lavagnini, I.R.; Campos, J.V.; Pallone, E.M.J.A. Microstructure evaluation of 3YSZ sintered by two-step flash sintering. *Ceram. Int.* **2021**, *47*, 21618–21624. [CrossRef]

22. Jansen, J.U.; Lümkemann, N.; Letz, I.; Pfefferle, R.; Sener, B.; Stawarczyk, B. Impact of high-speed sintering on translucency, phase content, grain sizes, and flexural strength of 3y-TZP and 4y-TZP zirconia materials. *J. Prosthet. Dent.* **2019**, *122*, 396–403. [CrossRef] [PubMed]

23. Kauling, A.E.; Güth, J.F.; Erdelt, K.; Edelhoff, D.; Keul, C. Influence of speed sintering on the fit and fracture strength of 3-unit monolithic zirconia fixed partial dentures. *J. Prosthet. Dent.* **2020**, *124*, 380–386. [CrossRef]

24. Denkena, B.; Breidenstein, B.; Busemann, S.; Lehr, C.M. Impact of hard machining on zirconia based ceramics for dental applications. *Procedia CIRP* **2017**, *65*, 248–252. [CrossRef]

25. Oghbaei, M.; Mirzaee, O. Microwave versus conventional sintering: A review of fundamentals, advantages and applications. *J. Alloys Compd.* **2010**, *494*, 175–189. [CrossRef]

26. Luz, J.N.; da Rosa Kaizer, M.; de Carvalho Ramos, N.; Anami, L.C.; Thompson, V.P.; Saavedra, G.D.S.F.A.; Zhang, Y. Novel speed sintered zirconia by microwave technology. *Dent. Mater.* **2021**, *37*, 875–881. [CrossRef]

27. Ahsanzadeh-Vadeqani, M.; Razavi, R.S. Spark plasma sintering of zirconia-doped yttria ceramic and evaluation of the microstructure and optical properties. *Ceram. Int.* **2016**, *42*, 18931–18936. [CrossRef]

28. Salamon, D.; Maca, K.; Shen, Z. Rapid sintering of crack-free zirconia ceramics by pressure-less spark plasma sintering. *Scr. Mater.* **2012**, *66*, 899–902. [CrossRef]

29. Fregeac, A.; Ansart, F.; Selezneff, S.; Estournès, C. Relationship between mechanical properties and microstructure of yttria stabilized zirconia ceramics densified by spark plasma sintering. *Ceram. Int.* **2019**, *45*, 23740–23749. [CrossRef]

30. Yousry, M.A.; Hammad, I.A.; El Halawani, M.T.; Aboushelib, M.N. Effect of sintering time on microstructure and optical properties of yttria-partially stabilized monolithic zirconia. *Dent. Mater.* **2023**, *39*, 1169–1179. [CrossRef]

31. Jerman, E.; Wiedenmann, F.; Eichberger, M.; Reichert, A.; Stawarczyk, B. Effect of high-speed sintering on the flexural strength of hydrothermal and thermo-mechanically aged zirconia materials. *Dent. Mater.* **2020**, *36*, 1144–1150. [CrossRef]

32. Al-Haj Husain, N.; Özcan, M.; Dydyk, N.; Joda, T. Conventional, speed sintering and high-speed sintering of zirconia: A systematic review of the current status of applications in dentistry with a focus on precision, mechanical and optical parameters. *JCM* **2022**, *11*, 4892. [CrossRef]

33. Chao, M.; Ning, L.; Zhikai, W.; Jing, T.; Jiazhen, Y. Influence on microstructure of dental zirconia ceramics prepared by two-step sintering. *West. China J. Stomatol.* **2013**, *31*, 496–499. [CrossRef]

34. Mazaheri, M.; Simchi, A.; Golestani-Fard, F. Densification and grain growth of nanocrystalline 3y-tzp powder compacts during two-step sintering. In Proceedings of the 2nd Conference on Nanostructure, Kish University, Kish Island, Iran, 11–14 March 2008.

35. Liu, W.L. *Advanced Ceramic Processing*, 1st ed.; Wuhan University of Technology Press: Wuhan, China, 2004.

36. Grech, J.; Antunes, E. Optimization of two-step sintering conditions of zirconia blanks for dental restorations. *Ceram. Int.* **2020**, *46*, 24792–24798. [CrossRef]

37. Chen, I.W.X. Sintering dense nanocrystalline ceramics without final-stage grain growth. *Nature* **2000**, *404*, 168–171. [CrossRef]

38. Wang, S.F.; Zhang, J.; Luo, D.W.; Gu, F.; Tang, D.Y.; Dong, Z.L.; Tan, G.E.; Que, W.X.; Zhang, T.S.; Li, S.; et al. Transparent ceramics: Processing, materials and applications. *Prog. Solid. State Chem.* **2013**, *41*, 20–54. [CrossRef]

39. Rajabi, J.; Muhamad, N.; Sulong, A.B. Effect of nano-sized powders on powder injection molding: A review. *Microsyst. Technol.* **2012**, *18*, 1941–1961. [CrossRef]

40. Olevsky, E.A. *Field-Assisted Sintering: Science and Applications*; Springer International Publishing AG: Cham, Switzerland, 2018.

41. Hu, Z.Y.; Zhang, Z.H.; Cheng, X.W.; Wang, F.C.; Zhang, Y.F.; Li, S.L. A review of multi-physical fields induced phenomena and effects in spark plasma sintering: Fundamentals and applications. *Mater. Des.* **2020**, *191*, 108662. [CrossRef]

42. Kang, S.L. What we should consider for full densification when sintering. *Materials* **2020**, *13*, 3578. [CrossRef]

43. Tran, T.B. Electric Field-Assisted Sintering of Nanocrystalline Hydroxyapatite for Biomedical Applications. Ph.D. Thesis, University of California, Oakland, CA, USA, 2010.

44. Ahmed, W.M.; Troczynski, T.; McCullagh, A.P.; Wyatt, C.C.; Carvalho, R.M. The influence of altering sintering protocols on the optical and mechanical properties of zirconia: A review. *J. Esthet. Restor. Dent.* **2019**, *31*, 423–430. [CrossRef] [PubMed]

45. Lubauer, J.; Schuenemann, F.H.; Belli, R.; Lohbauer, U. Speed-sintering and the mechanical properties of 3–5 mol% y2o3-stabilized zirconias. *Odontology* **2023**, *111*, 883–890. [CrossRef] [PubMed]

46. Groza, J.R.; Zavaliangos, A. Sintering activation by external electrical field. *Mater. Sci. Eng. A Struct. Mater. Prop. Microstruct. Process.* **2000**, *287*, 171–177. [CrossRef]

47. Grasso, S.; Sakka, Y.; Maizza, G. Electric current activated/assisted sintering (ECAS): A review of patents 1906–2008. *Sci. Technol. Adv. Mater.* **2009**, *10*, 53001. [CrossRef] [PubMed]

48. Wei, X.; Back, C.; Izhvanov, O.; Haines, C.D.; Olevsky, E.A. Zirconium carbide produced by spark plasma sintering and hot pressing: Densification kinetics, grain growth, and thermal properties. *Materials* **2016**, *9*, 577. [CrossRef]

49. Zhang, J.; Zavaliangos, A.; Groza, J.R. Field activated sintering techniques: A comparison and contrast. *P/M Sci. Technol. Briefs* **2003**, *5*, 17–21.

50. Yang, C.C.; Ding, S.J.; Lin, T.H.; Yan, M. Mechanical and optical properties evaluation of rapid sintered dental zirconia. *Ceram. Int.* **2020**, *46*, 26668–26674. [CrossRef]

51. Suárez, M.; Fernández, A.; Menéndez, J.L.; Torrecillas, R.; Kessel, H.U.; Hennicke, J. Challenges and opportunities for spark plasma sintering: A key technology fora new generation of materials. In *Sintering Applications*; InTech: Nappanee, IN, USA, 2013.

52. Lawson, N.C.; Maharishi, A. Strength and translucency of zirconia after high-speed sintering. *J. Esthet. Restor. Dent.* **2020**, *32*, 219–225. [CrossRef]

53. Sulaiman, T.A.; Abdulmajeed, A.A.; Donovan, T.E.; Vallittu, P.K.; Närhi, T.O.; Lassila, L.V. The effect of staining and vacuum sintering on optical and mechanical properties of partially and fully stabilized monolithic zirconia. *Dent. Mater. J.* **2015**, *34*, 605–610. [CrossRef]

54. Kaizer, M.R.; Gierthmuehlen, P.C.; Dos Santos, M.B.; Cava, S.S.; Zhang, Y. Speed sintering translucent zirconia for chairside one-visit dental restorations: Optical, mechanical, and wear characteristics. *Ceram. Int.* **2017**, *43*, 10999–11005. [CrossRef]

55. Stawarczyk, B.; Özcan, M.; Hallmann, L.; Ender, A.; Mehl, A.; Hämmerlet, C.H. The effect of zirconia sintering temperature on flexural strength, grain size, and contrast ratio. *Clin. Oral. Investig.* **2013**, *17*, 269–274. [CrossRef]

56. Lee, S.; Choi, G.; Choi, J.; Kim, Y.; Kim, H.K. Effect of high-speed sintering on the marginal and internal fit of CAD/CAM-fabricated monolithic zirconia crowns. *Sci. Rep.* **2023**, *13*, 17215. [CrossRef]

57. Rybakov, K.I.; Olevsky, E.A.; Krikun, E.V. Microwave sintering: Fundamentals and modeling. *J. Am. Ceram. Soc.* **2013**, *96*, 1003–1020. [CrossRef]

58. Amikam Birnboim, D.G.L.C. Comparative study of microwave sintering of zinc oxide at 2.45, 30, and 83 GHz. *I. Am. Ceram. Soc.* **1998**, *81*, 1493–1501. [CrossRef]

59. Wang, J.; Binner, J.; Vaidhyanathan, B.; Joomun, N.; Kilner, J.; Dimitrakis, G.; Cross, T.E. Evidence for the microwave effect during hybrid sintering. *J. Am. Ceram. Soc.* **2006**, *89*, 1977–1984. [CrossRef]

60. Binner, J.; Annapoorani, K.; Paul, A.; Santacruz, I.; Vaidhyanathan, B. Dense nanostructured zirconia by two stage conventional/hybrid microwave sintering. *J. Eur. Ceram. Soc.* **2008**, *28*, 973–977. [CrossRef]

61. Aman, B.; Acharya, S.; Reeja Jayan, B. Making the case for scaling up microwave sintering of ceramics. *Adv. Eng. Mater.* **2024**, *26*, 2302065. [CrossRef]

62. Menezes, R.R.; Kiminami, R.H.G.A. Microwave sintering of alumina–zirconia nanocomposites. *J. Mater. Process. Technol.* **2008**, *203*, 513–517. [CrossRef]

63. Ersoy, N.M.; Aydoğdu, H.M.; Değirmenci, B.Ü.; Çökük, N.; Sevimay, M. The effects of sintering temperature and duration on the flexural strength and grain size of zirconia. *Acta Biomater. Odontol. Scand.* **2015**, *1*, 43–50. [CrossRef]

64. Aziz, A.G.A. The Effect of Artificial Aging (LTD) on the Mechanical and Optical Properties of Conventional and Translucent Zirconia for Fixed Prosthodontics. Ph.D. Thesis, University of Leeds, Leeds, UK, 2018.

65. Liu, H.; Inokoshi, M.; Xu, K.; Tonprasong, W.; Minakuchi, S.; Van Meerbeek, B.; Vleugels, J.; Zhang, F. Does speed-sintering affect the optical and mechanical properties of yttria-stabilized zirconia? A systematic review and meta-analysis of in-vitro studies. *Jpn. Dent. Sci. Rev.* **2023**, *59*, 312–328. [CrossRef]

66. Salah, K.; Sherif, A.H.; Mandour, M.H.; Nossair, S.A. Optical effect of rapid sintering protocols on different types of zirconia. *J. Prosthet. Dent.* **2023**, *130*, 251–253. [CrossRef]

67. Zhang, F.; Inokoshi, M.; Batuk, M.; Hadermann, J.; Naert, I.; Van Meerbeek, B.; Vleugels, J. Strength, toughness and aging stability of highly-translucent y-TZP ceramics for dental restorations. *Dent. Mater.* **2016**, *32*, e327–e337. [CrossRef]

68. Ebeid, K.; Wille, S.; Hamdy, A.; Salah, T.; El-Etreby, A.; Kern, M. Effect of changes in sintering parameters on monolithic translucent zirconia. *Dent. Mater.* **2014**, *30*, e419–e424. [CrossRef]

69. Jiang, L.; Liao, Y.; Wan, Q.; Li, W. Effects of sintering temperature and particle size on the translucency of zirconium dioxide dental ceramic. *J. Mater. Sci. Mater. Med.* **2011**, *22*, 2429–2435. [CrossRef]

70. Almazdi, A.A.; Khajah, H.M.; Monaco Jr, E.A.; Kim, H. Applying microwave technology to sintering dental zirconia. *J. Prosthet. Dent.* **2012**, *108*, 304–309. [CrossRef]

71. Huang, W.; Qiu, H.; Zhang, Y.; Zhang, F.; Gao, L.; Omran, M.; Chen, G. Microstructure and phase transformation behavior of al2o3–ZrO2 under microwave sintering. *Ceram. Int.* **2023**, *49*, 4855–4862. [CrossRef]

72. Arellano Moncayo, A.M.; Peñate, L.; Arregui, M.; Giner-Tarrida, L.; Cedeño, R. State of the art of different zirconia materials and their indications according to evidence-based clinical performance: A narrative review. *Dent. J.* **2023**, *11*, 18. [CrossRef]

73. Camposilvan, E.; Leone, R.; Gremillard, L.; Sorrentino, R.; Zarone, F.; Ferrari, M.; Chevalier, J. Aging resistance, mechanical properties and translucency of different yttria-stabilized zirconia ceramics for monolithic dental crown applications. *Dent. Mater.* **2018**, *34*, 879–890. [CrossRef]

74. Ji, M.; Xu, J.; Yu, D.; Chen, M.; El Mansori, M. Influence of sintering temperatures on material properties and corresponding milling machinability of zirconia ceramics. *J. Manuf. Process.* **2021**, *68*, 646–656. [CrossRef]

75. Fan, D.; Chen, L. Computer simulation of grain growth and ostwald ripening in alumina-zirconia two-phase composites. *J. Am. Ceram. Soc.* **1997**, *80*, 1773–1780. [CrossRef]

76. Ayata, M.; Albayrak, H.; Eraslan, R. Does fast sintering affect the optical properties, fracture strength, and microstructure of monolithic zirconia? *Odontology* **2025**. [CrossRef] [PubMed]

77. Kulyk, V.; Duriagina, Z.; Vasyliv, B.; Kovbasiuk, T.; Lyutyy, P.; Vira, V.; Vavrukh, V. Effect of sintering temperature on crack growth resistance characteristics of yttria-stabilized zirconia. *Acta Phys. Pol. A* **2022**, *141*, 323–327. [CrossRef]

78. Chen, P.; Li, X.; Tian, F.; Liu, Z.; Hu, D.; Xie, T.; Liu, Q.; Li, J. Fabrication, microstructure, and properties of 8 mol% yttria-stabilized zirconia (8YSZ) transparent ceramics. *J. Adv. Ceram.* **2022**, *11*, 1153–1162. [CrossRef]

79. Huang, Z.; Wang, L.; Dou, R. Ultrafast high-temperature sintering of 3d-printed yttria-stabilized zirconia: Microstructure and mechanical insights. *Ceram. Int.* **2025**, *51*, 43125–43136. [CrossRef]

80. Cokic, S.M.; Vleugels, J.; Van Meerbeek, B.; Camargo, B.; Willems, E.; Li, M.; Zhang, F. Mechanical properties, aging stability and translucency of speed-sintered zirconia for chairside restorations. *Dent. Mater.* **2020**, *36*, 959–972. [CrossRef]

81. Chevalier, J.; Cales, B.; Drouin, J.M. Low-temperature aging of y-TZP ceramics. *J. Am. Ceram. Soc.* **1999**, *82*, 2150–2154. [CrossRef]

82. Ramesh, S.; Sara Lee, K.Y.; Tan, C.Y. A review on the hydrothermal ageing behaviour of y-TZP ceramics. *Ceram. Int.* **2018**, *44*, 20620–20634. [CrossRef]

83. Cattani-Lorente, M.; Durual, S.; Amez-Droz, M.; Wiskott, H.A.; Scherrer, S.S. Hydrothermal degradation of a 3y-TZP translucent dental ceramic: A comparison of numerical predictions with experimental data after 2 years of aging. *Dent. Mater.* **2016**, *32*, 394–402. [CrossRef]

84. Guo, X.; He, J. Hydrothermal degradation of cubic zirconia. *Acta Mater.* **2003**, *51*, 5123–5130. [CrossRef]

85. Kohal, R.; Douillard, T.; Sanon, C.; Kocjan, A.; Chevalier, J. Signs of in-vivo aging of zirconia from explanted dental implants with porous coating after several years in function. *Acta Biomater.* **2025**, *194*, 498–513. [CrossRef] [PubMed]

86. Aragón-Duarte, M.C.; Nevarez-Rascón, A.; Esparza-Ponce, H.E.; Nevarez-Rascón, M.M.; Talamantes, R.P.; Ornelas, C.; Mendez-Nonell, J.; González-Hernández, J.; Yacamán, M.J.; Hurtado-Macías, A. Nanomechanical properties of zirconia- yttria and alumina zirconia- yttria biomedical ceramics, subjected to low temperature aging. *Ceram. Int.* **2017**, *43*, 3931–3939. [CrossRef]

87. Ban, S.; Sato, H.; Suehiro, Y.; Nakanishi, H.; Nawa, M. Biaxial flexure strength and low temperature degradation of Ce-TZP/Al_2O_3 nanocomposite and y-TZP as dental restoratives. *J. Biomed. Mater. Res.* **2008**, *87B*, 492–498. [CrossRef]

88. Chevalier, J. Critical effect of cubic phase on aging in 3mol% yttria-stabilized zirconia ceramics for hip replacement prosthesis. *Biomaterials* **2004**, *25*, 5539–5545. [CrossRef]

89. Kocjan, A.; Cotič, J.; Kosmač, T.; Jevnikar, P. In vivo aging of zirconia dental ceramics—Part i: Biomedical grade 3y-TZP. *Dent. Mater.* **2021**, *37*, 443–453. [CrossRef]

90. Cotič, J.; Kocjan, A.; Panchevska, S.; Kosmač, T.; Jevnikar, P. In vivo ageing of zirconia dental ceramics—part II: Highly-translucent and rapid-sintered 3y-TZP. *Dent. Mater.* **2021**, *37*, 454–463. [CrossRef]

91. Pereira, G.K.R.; Venturini, A.B.; Silvestri, T.; Dapieve, K.S.; Montagner, A.F.; Soares, F.Z.M.; Valandro, L.F. Low-temperature degradation of y-TZP ceramics: A systematic review and meta-analysis. *J. Mech. Behav. Biomed. Mater.* **2016**, *55*, 151–163. [CrossRef] [PubMed]

92. Sutharsini, U.; Thanihaichelvan, M.; Ting, C.H.; Ramesh, S.; Tan, C.Y.; Chandran, H.; Sarhan, A.A.; Urriés, I. Effect of two-step sintering on the hydrothermal ageing resistance of tetragonal zirconia polycrystals. *Ceram. Int.* **2017**, *43*, 7594–7599. [CrossRef]

93. Kongkiatkamon, S.; Peampring, C. Effect of speed sintering on low temperature degradation and biaxial flexural strength of 5y-TZP zirconia. *Molecules* **2022**, *27*, 5272. [CrossRef] [PubMed]
94. Uwanyuze, R.S.; Ramesh, S.; King, M.K., Jr.; Lawson, N.; Mahapatra, M.K. Mechanical properties, translucency, and low temperature degradation (LTD) of yttria (3–6 mol%) stabilized zirconia. *Ceram. Int.* **2021**, *47*, 15868–15874. [CrossRef]